# Phase Morphology of Polystyrene–Polyarylate Block Copolymer/Polycarbonate Blends and Their Application to Disk Substrates

**HIROSHI OHISHI,[1] TAKAYUKI IKEHARA,[2] TOSHIO NISHI[2]**

[1] Advanced Technology Research Laboratories, Nippon Steel Corporation, 20-1 Shintomi, Futtsu, Chiba 293-8511, Japan

[2] Department of Applied Physics, School of Engineering, the University of Tokyo, 7-3-1 Hongo, Bunkyo-ku, Tokyo 113-8656, Japan

*Received 4 October 2000; accepted 10 December 2000*

**ABSTRACT:** Polystyrene–polyarylate (PS–PAr) block copolymer was applied as a moldability modifier of polycarbonate (PC). From the 1,1,1,3,3,3-hexafluoro-2-propanol (HFIP) extraction results, PS–PAr block copolymer was demonstrated to copolymerize with PC via an *in situ* reaction between the PAr chain and PC. As a result of the chemical bonding between PS and PC chains, the PS dispersed domain in the PS–PAr block copolymer/PC blend could be reduced, on average, to a size smaller than the visible light wavelength. In particular, by adjusting PAr composition to 30 wt % in the fed PS–PAr block copolymer during the melt-mixing process, the PS domain size was completely reduced to be smaller than the visible light wavelength. As a result the blend substrate could satisfy the transparency required for the optical disk substrate with higher memory density: homogeneity under polarizing light, clarity on the reflective plate, and transparency at 400 nm. The melt viscosity could be lowered to the equal viscosity level of PC at about 30°C higher temperature by blending PC 15 wt % with the PS–PAr block copolymer. The lowered melt viscosity could reduce the retardation in the optical disk substrate, which was equivalent to that of the PC substrate processed at 30°C higher. In addition, the PS–PAr block copolymer/PC blend could attain the exact groove transcription at 20°C lower mold temperature than that of PC as a result of the lowered elastic modulus caused by the PS-rich phase. These features of the PS–PAr block copolymer/PC blend indicated a potential to offer an improved process window for the substrate molding. Because of its excellent transparency and a potential for processing flexibility, the PS–PAr block copolymer/PC blend would be a promising material for optical disk substrates with higher memory density.  J Appl Polym Sci 82: 2566–2582, 2001

**Key words:** polystyrene; polyarylate; block copolymer; polycarbonate; transesterification; reactive processing; optical disk; transmissivity; birefringence; transcription

## INTRODUCTION

Molecular design of reactive polymers and block or graft copolymers has been one of the major topics in both polymer science and industry during the last two decades. Block or graft copolymers, in which different polymer segments are chemically bonded together, have been known to have additional properties that are different from those of each polymer. Furthermore, because of their microdomain structure it has been made clear that block copolymers exhibit their own

*Correspondence to:* H. Ohishi (hohishi@re.nsc.co.jp).

Journal of Applied Polymer Science, Vol. 82, 2566–2582 (2001)

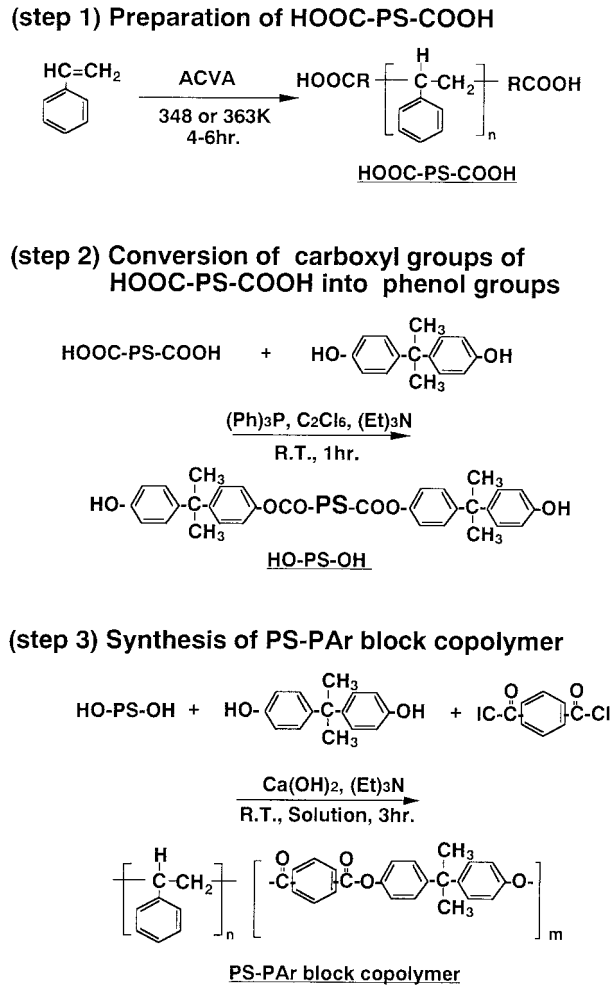


**Figure 1** Reaction scheme for synthesis of PS–PAr block copolymer.

unique characteristics. Many important applications have been found for block or graft copolymers in the polymer industry. For example, a block or a graft copolymer can be utilized by itself as a high-performance polymer, or be added as a surface modifier for polymeric materials or a compatibilizer for mechanical blends of two immiscible polymer blend systems.[1–5]

We carried out research and development on polystyrene–polyarylate (PS–PAr) block copolymers.[6–12] In our earlier publications, we proposed a novel synthetic procedure of PS–PAr block copolymer utilizing a telechelic PS (Fig. 1).[6–8] We also previously reported its high potential for optical applications[6,7,9] and for a compatibilizer for an immiscible blend system of high-impact polystyrene (HIPS) and polycarbonate (PC).[11,12]

In this research, we have attempted to apply PS–PAr block copolymer as a moldability modifier for PC, which is an important engineering polymer used in a wide variety of applications because of its excellent balance of properties including optical clarity, high heat deformation temperature, mechanical properties, toughness, and electrical properties. However, PC has some deficient characteristics that deter its use in some areas. Poor moldability is one of the most serious of PC's defects that make it difficult to utilize PC for a substrate of optical-data disk with higher memory density.[13–21] For higher memory density optical data storage systems, pits or grooves, which record or address the memory, should be replicated on the substrate surface with the finer feature and at the narrower track pitches.[13–17] In addition, as the size and the spacing of the pits or grooves become smaller, reduction of birefringence becomes increasingly important to maintain the required signal/noise level.[13,17–21] Poor moldability of PC has restricted the process window to extremely high melt temperatures and mold temperatures, even for the standard substrate molding. Little process flexibility is allowed for the substrate molding with higher memory density disks. To accommodate these stringent requirements, the moldability of PC should be improved.

Polystyrene (PS) is a transparent polymer with excellent moldability, although its mechanical properties are significantly inferior to those of PC. Thus the focus of our research is to improve the moldability of PC by blending PS and PC, and produce a high-performance polymer with high mechanical properties and an improved process window for the disk substrate molding. However, because PS and PC are immiscible,[22–29] simple mechanical blending of these polymers makes it difficult to control the domain structure on a microscopic level. For the optical disk substrates, the domain size should be controlled to be smaller than the visible light wavelength, to prevent the light scattering caused by the dispersed domains. In that way, incorporation of chemical bonds between PC and PS molecules is a good method. In this research we paid attention to the experimental results that PAr undergoes transesterification with PC via an *in situ* reaction.[30] By making use of PAr chains in PS–PAr block copolymers as a reactive unit to PC and blending them in an extruder, PS and PC could be copolymerized in a block form during the blend preparation via transesterification between the PAr chains and PC.

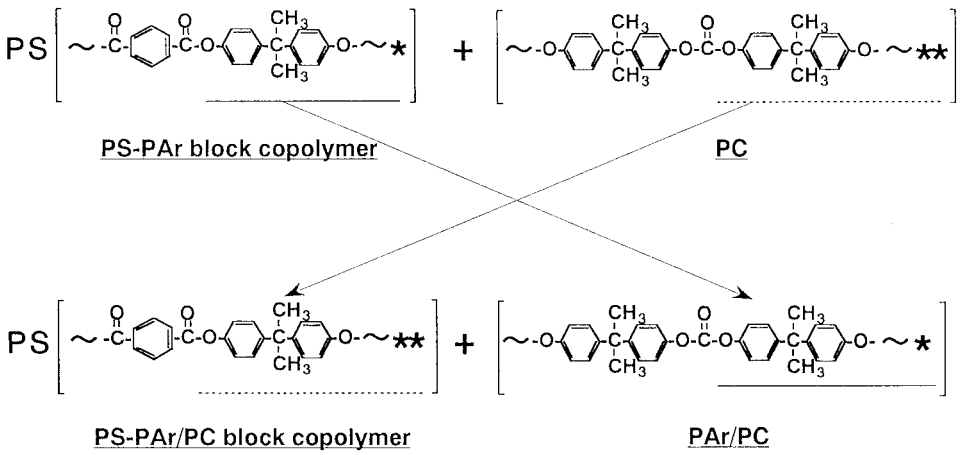


**Figure 2** Transesterification between PS–PAr block copolymer and PC.

The purpose of this investigation is to confirm the transesterification between PS–PAr block copolymer and PC and to investigate the relationship between the micromorphologies and the transparency of these blends. In addition, the retardation and the groove transcription of the PS–PAr block copolymer/PC blend disk substrates were also investigated.

### Reaction Scheme Between PS–PAr Block Copolymer and PC via *in Situ* Reaction

Figure 2 gives the expected *in situ* reaction scheme between PS–PAr block copolymer and PC during the extrusion process. Unlike the case for the polyamide-based[31–33] or polyester-based[34–37] polymer blends, schemes for formation of a block or a graft polymer by *in situ* reaction with PC are not popular, although a few schemes have been reported so far. This is mainly because of the fact that the terminal phenol groups of PC chains are usually capped for prevention of the Fries transition.[38] As a result, the terminal functional groups of PC chain cannot be utilized as reactive units like polyesters or polyamides.

Wildes et al.[39–41] proposed an *in situ* reaction scheme between the amine group–introduced SAN (styrene–acrylonitrile random copolymer) and PC. In this procedure, the SAN was copolymerized with PC in a graft form via *trans*-reaction between the amine groups in SAN and the carbonate bonds in PC. This scheme appears to be excellent for *in situ* reaction to generate a graft copolymer of PS or SAN and PC for the following two reasons: (1) the amine groups are relatively easily introduced into PS or SAN chain through the reaction between 1-(2-aminoethyl)piperazine and maleic anhydride–introduced PS or SAN[40]; (2) the amine group in PS or SAN can react with PC even if end capped. However, this scheme is lacking in chemical stability because phenol-terminated PC is generated as a result of the *trans*-reaction between the amine groups and the carbonate units.[40]

On the other hand, the reaction scheme of Figure 2 can overcome all of the aforementioned problems. PAr chains in PS–PAr block copolymer can react with PC even if end capped. In addition, all products in Figure 2 have high chemical stability. No phenol-terminated PC is generated. Furthermore, aliphatic carbonates such as ethylene or butylene carbonate are not generated through the transesterification of Figure 2. These kinds of aliphatic carbonates are poor in thermal stability, although they are usually generated in widely commercialized polymer blend systems of PC and poly(ethylene terephthalate) (PET) or poly(butylene terephthalate) (PBT) through the transesterification between PC and PET[42,43] or PBT.[44–46]

## EXPERIMENTAL

### Materials and Blend Compositions

In this research, PAr chains in PS–PAr block copolymer were utilized just as a reactive unit to PC. Thus, the PAr wt % in the PS–PAr block copolymer was designed to be as small as possible. The minimum PAr wt % in the PS–PAr block

**Table I Synthesis and Characterization of PS–PAr Block Copolymer**

| | Feed | | | PS–PAr Block Copolymer | | | | | |
|---|---|---|---|---|---|---|---|---|---|
| | HOOC–PS–COOH | | | | | | | Pure PS–PAr Block Copolymer[b] | |
| Run[a] | $M_n$ | $M_w$ | PS–PAr (wt %) | $M_n$[c] | $M_w$[c] | homo-PS[b] (wt %) | homo-PAr (wt %) | (wt %) | PS–PAr |
| 2185 | 21,000 | 50,000 | 85/15 | 32,000 | 85,000 | — (10.1) | ~ 0 (0.6) | — (89.4) | — (84/16) |
| 870 | 7,500 | 12,000 | 70/30 | 14,000 | 40,000 | — (8.4) | 3.5 (1.2) | — (90.4) | — (68/32) |
| 2170 | 21,000 | 50,000 | 70/30 | 14,000 | 40,000 | — (6.3) | 5.0 (6.0) | — (87.7) | — (73/27) |

[a] The first two digits correspond to the $M_n$ of the fed COOH–PS–COOH, and the last two digits correspond to the wt % of the fed HOOC–PS–COOH.
[b] $M_n$ and $M_w$ of PS–PAr block copolymer were measured without any purification.
[c] The wt % values in parentheses were predicted by the kinetic simulation model.[8]

copolymer was determined by eq. (1) corresponding to the $M_n$ of the fed HOOC–PS–COOH:

$$\text{PAr wt \%} = 10M_{\text{PAr}}/(M_{n\,\text{HOOC–PS–COOH}} + 10M_{\text{PAr}}) \quad (1)$$

where $M_{\text{PAr}}$ is the molecular weight of the PAr unit, 358 g/mol. The amount of the fed bisphenol A (BPA) determined by eq. (1) corresponded to the minimum amount (10 times higher amount than the stoichiometric amount of BPA in step 2 of Fig. 1) that was required for the suppression of the intermolecular coupling between HOOC–PS–COOH molecules in step 2.[7] By feeding this amount of BPA in step 2 and synthesizing PS–PAr block copolymer consecutively from step 2 to step 3 of Figure 1, PS–PAr block copolymer could be obtained without any coupling between HOOC–PS–COOH molecules and any loss in the fed BPA.[7]

The PS–PAr block copolymers of Table I were synthesized (Fig. 1) and characterized according to the same procedure described previously.[7] The PAr wt % in the runs 2185 and the 0870 corresponded to the minimum wt % determined by eq. (1). The PC was Panlite AD5530 (obtained from Teijin Chemical Industry, Tokyo, Japan), which was a low molecular weight PC designed for optical disk application. The number-and the weight-average molecular weights ($M_n$ and $M_w$) of this PC were15,000 and 25,000, respectively.

In the following analysis, the blend composition of the PS–PAr block copolymer/PC was kept 15/85 (by weight) on the basis of the experimental results of Figure 3. The critical point was found around 15 wt %, where the tensile strength of PS–PAr block copolymer/PC blend changed from equal to half level of PC (Fig. 3).

### Melt Processing and Injection Molding

The 15/85 blends of HOOC–PS–COOH/PC and the PS–PAr block copolymer/PC were premixed by V-shaped dry blender and then intensively melt mixed by a corotating twin-screw extruder (TEX30SS, 30-mm diameter, L/D = 50; Japan Steel Making Works, Hiroshima, Japan) at 120 rpm and a barrel temperature of 260°C. The average shear rate and the mixing time during the

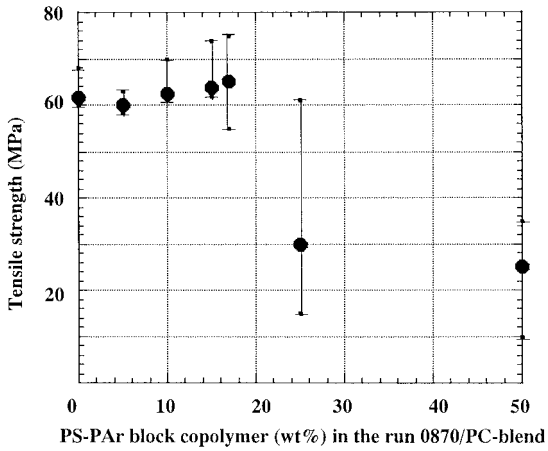


**Figure 3** Tensile strength of the run 0870/PC blends as a function of the PS–PAr block copolymer composition. The experimental error bar shows the range of data, excluding the maximum and minimum values.

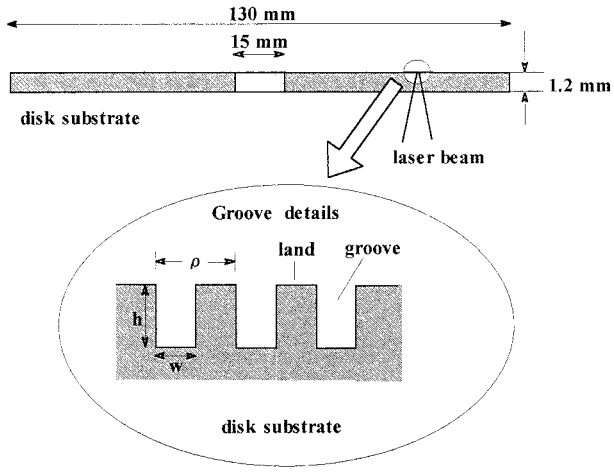


**Figure 4** A cross section of a disk substrate with an enlarged schematic view of the groove profiles. The periodicity $\rho$, depth $h$, and width $w$ were 1.6 $\mu$m, 110 nm, and 0.55 $\mu$m, respectively.

extrusion process were kept at about 225 $s^{-1}$ and 2 min, respectively. Disk substrates (Fig. 4; Table II) of these blends were injection molded using a M-70A-D-DM injection-molding machine (Meiki, Nagoya, Japan). The minute grooves of Figure 4 were replicated on the substrate surface from a stamper inserted in the mold. The molding conditions in Table III were kept constant through all the experiments. Only for the purpose of examining the effect of the melt temperature or the mold temperature on the retardation or the groove transcription were they varied from 300°C to 370°C and from 80°C to 120°C, respectively.

### Confirmation of the Reactivity Between the PS–PAr Block Copolymers and PC

The blends of PS–PAr block copolymer (Table I) and PC thus extruded were solved into chloroform and poured into methanol to precipitate the powdered sample. The precipitates were collected by filtration, washed 10 times with methanol, and dried in a vacuum dryer at 80°C for 12 h, after which they were fractionated by Soxhlet extraction with 1,1,1,3,3,3-hexafluoro-2-propanol (HFIP) for 96 h. Chemical composition of both the HFIP solubles and insolubles was determined by proton nuclear magnetic resonance ($^1$H–NMR) spectrum in $CDCl_3$ solution using JEOL JP, JNM-EX40 (JEOL, Peabody, MA).

As preliminary experiments, only the PS–PAr block copolymers in Table I were melt mixed, recovered, and fractionated with HFIP in the aforementioned way. Then the mass balance and the chemical composition of both HFIP solubles and insolubles were compared before and after the melt mixing. The results of these preliminary experiments revealed that their mass balance and the chemical composition were almost the same before and after the melt mixing. These results indicated that the solubility behavior of the PS–PAr block copolymers to HFIP never changed by melt mixing them alone under these conditions.

### Observation of Phase Morphologies and Measurements of Optical Properties, Melt Viscosity, Degree of Groove Replication, and Viscoelastic Properties

The blend morphologies were examined by a scanning electron microscope (SEM) or a transmission electron microscope (TEM) in the same way as previously described.[12] For both observations the specimens were cut from the core part of the radial section of the disk substrates. In the SEM micrographs, the darker portions are assigned to the PS-rich phases that are eliminated by the etchant, whereas the brighter portions are assigned to the PC-rich phases. In the TEM micrographs the darker portion was the PS-rich phase, which was selectively stained with ruthenium tetra-oxide. To measure the domain size and its distribution the SEM and the TEM micrographs were analyzed by digital image analysis. The domain sizes were estimated using the major axis of the equivalent ellipsoid.

Transmissivity of the disk substrates was measured spectroscopically using the light source storage systems with 800- and 400-nm wavelength, which were the same as the laser wave-

**Table II Injection-Molding Conditions for the Disk Substrates**

| Barrel Temperature (°C) | Mold Temperature (°C) | Injection Rate ($cm^3$/s) | Holding Pressure (MPa) | Holding Time (s) | Waiting Time Until Cutting Gate (s) |
|---|---|---|---|---|---|
| 340 | 100 | 20 | 30 | 1.0 | 0.5 |

**Table III Mass Balance of the HFIP Extractions**

| Sample | Feed (by weight) | Before the Melt Mixing | | After the Melt Mixing | |
|---|---|---|---|---|---|
| | | Solubles (wt %) | Insolubles (wt %) | Solubles (wt %) | Insolubles (wt %) |
| Run 0870/PC | 15/85 | 85.2 | 14.7 | 60.0 | 37.0 |
| Run 2170/PC | | 85.6 | 14.0 | 94.0 | 4.0 |
| Run 2185/PC | | 86.0 | 13.0 | 90.0 | 7.8 |

lengths used and proposed for the standard and the higher memory density optical data system,[13] respectively. The retardation of the substrates was measured by polarizing microscope equipped with a Senalmon-type compensator. The melt viscosity data were obtained by capillary viscometry using a Chapirograph 1B rheometer (Toyo Seiki Seisaku-Sho, Tokyo, Japan) with L/D = 20 (1-mm diameter). The extent of the groove transcription was measured by an atomic force microscope[15–17,47] (AFM; Nano Scope AFM, Digital Instruments, Santa Barbara, CA). For the AFM analysis, 10 × 10-mm pieces were cut from the outermost parts of the substrate, because the exact transcription of the grooves is reported to be more difficult toward the outside diameter.[13–17] The viscoelastic behavior was measured by dynamic mechanical measurement (d.m.s.) using a Rheovibron DDV-II dynamic tensile tester (Toyo Measuring Instruments, Tokyo, Japan) automated by Imass Inc. The data were obtained at 10 Hz and a heating rate of 2°C/min.

## RESULTS AND DISCUSSION

### Confirmation of the Reactivity Between PS–PAr Block Copolymer and PC

Given the similarity in the chemical structures between PAr and PC, there should be no major changes in the FTIR[30] or the NMR spectra of the bulk component before and after the transesterification of Figure 2. Thus, we have focused on the following experimental results. The solubility behavior of PS–PAr block copolymers changed from HFIP-insoluble to HFIP-soluble when the PAr wt % in PS–PAr block copolymer surpassed the critical point.[7] The critical points varied with the $M_n$ of the PS chain in PS–PAr block copolymer. When the $M_n$ of the PS chains in the PS–PAr block copolymer were 8000 and 21,000, they were around 50 and 75 wt %, respectively.[7] Because both PC and PAr were soluble to HFIP, the generated PS–PAr/PC block copolymer should change from HFIP-insoluble to HFIP-soluble if the wt % of the PAr/PC chains in the PS–PAr/PC block copolymer of Figure 2 surpassed these critical points. The reactivity of the scheme of Figure 2 was confirmed on the basis of this solubility behavior change before and after the reaction.

Table III and Figure 5 give the mass balance and the typical NMR spectra of both HFIP solubles and insolubles, both before and after the melt mixing, respectively. Before the melt mixing, the NMR spectra in the HFIP solubles and insolubles were all assigned to PC and PS–PAr block copolymer, respectively.[7] In addition, the amount of the HFIP solubles and insolubles was almost equal to that of the fed PC and the PS–PAr block copolymer, respectively. These results demonstrated that the fed PC and PS–PAr block copolymer could be almost completely fractionated by HFIP before the melt mixing.

On the other hand, after the extruding one can see clear changes in both NMR spectra and mass balance. In the NMR spectra of the HFIP solubles, one can see slight peaks at 7.5–6.2 ppm[7] and 9.0–7.5 ppm,[7,48] whereas in the HFIP insolubles, the NMR spectrum at 7.5–6.9 ppm[7,48] was increased. By combining these results with the preliminary experimental results and the expected change in the solubility behavior, these changes in the NMR spectra could be attributed to the following three kinds of reaction products in Figure 2:

1. PS–PAr/PC block copolymer with PAr/PC wt %, which was larger than the critical point.
2. PS–PAr/PC block copolymer with PAr/PC wt %, which was smaller than the critical point.
3. PAr/PC copolymer.

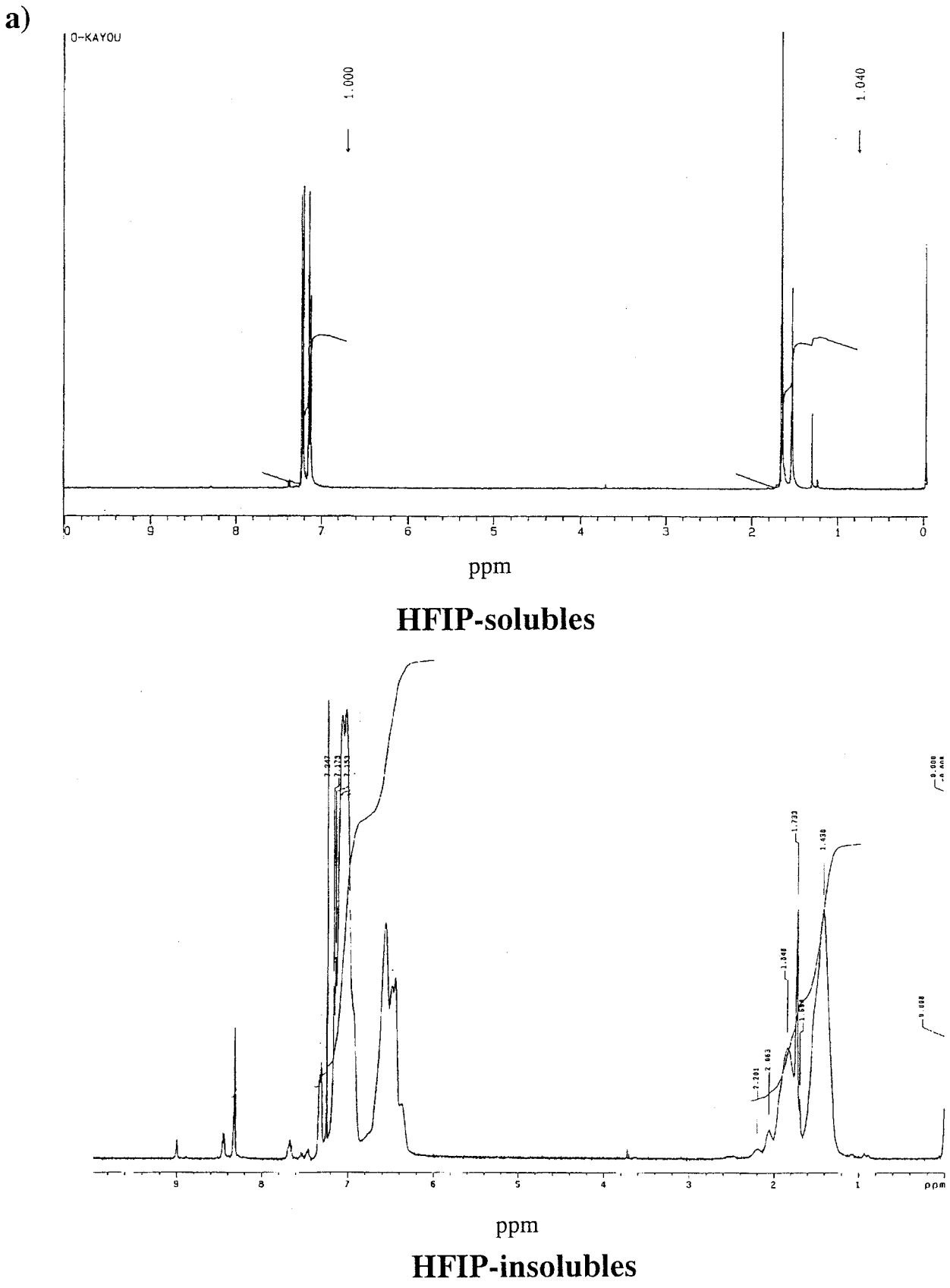


**Figure 5** $^{1}$H–NMR spectra of HFIP solubles and insolubles of the run 0870/PC blend, before (a) and after (b) melt mixing.

b)

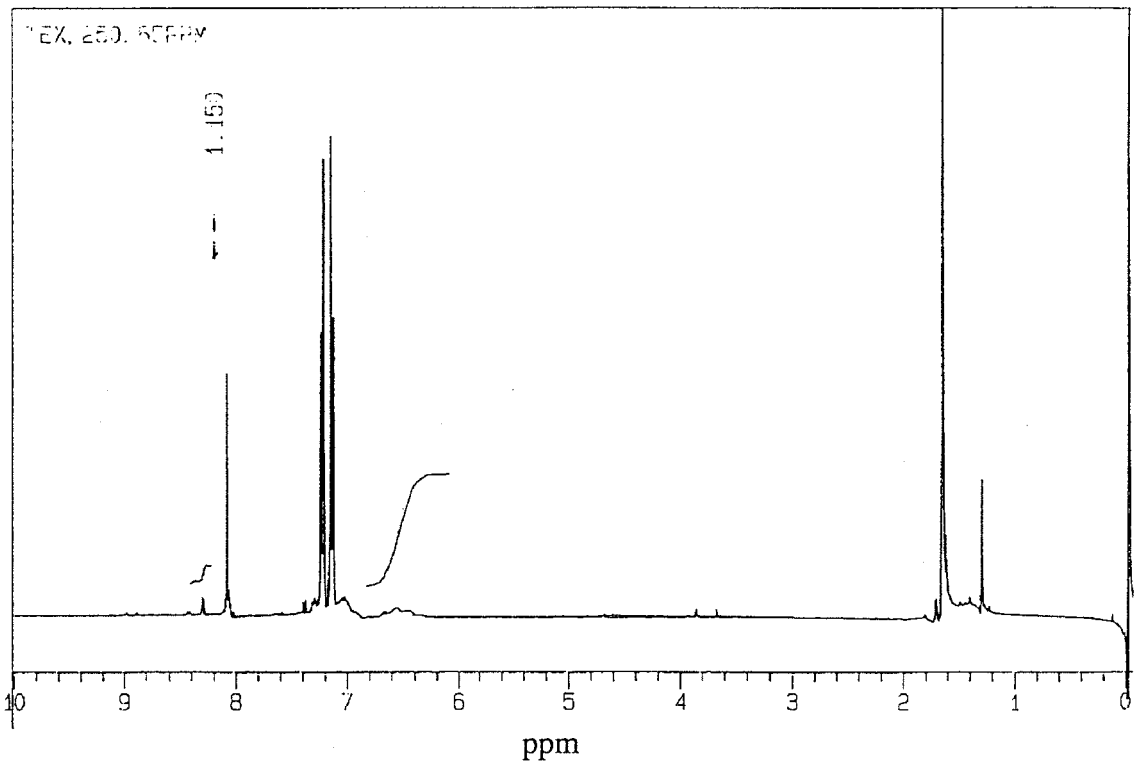


HFIP-solubles

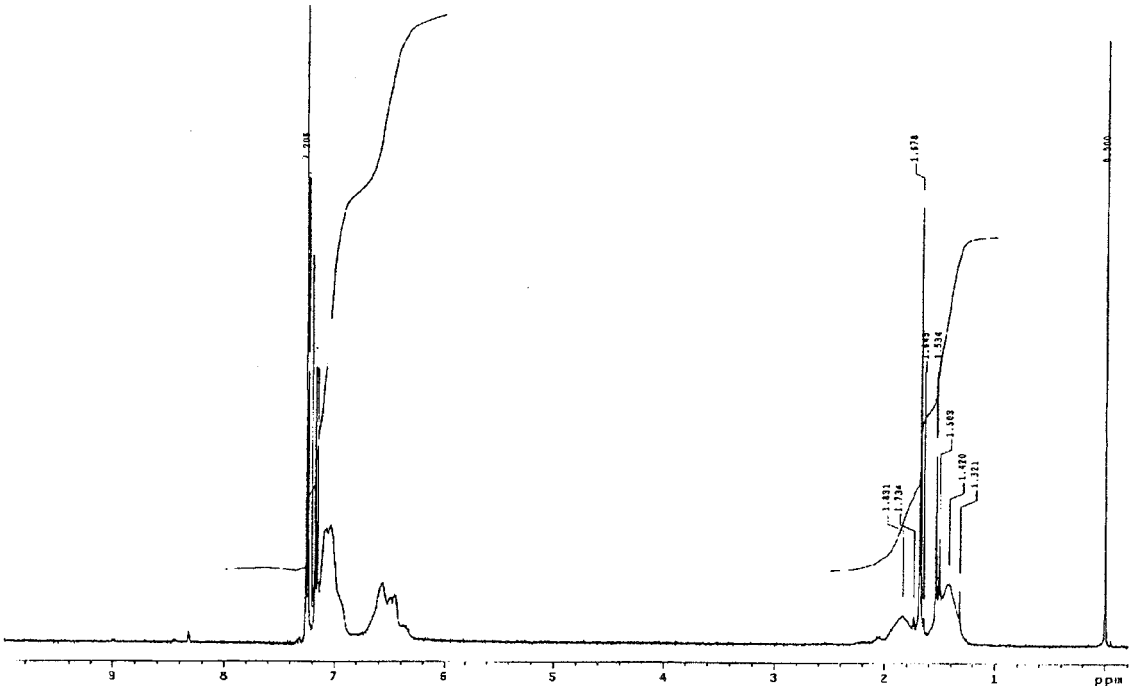


ppm

HFIP-insolubles

**Figure 5** (*Continued from the previous page*)

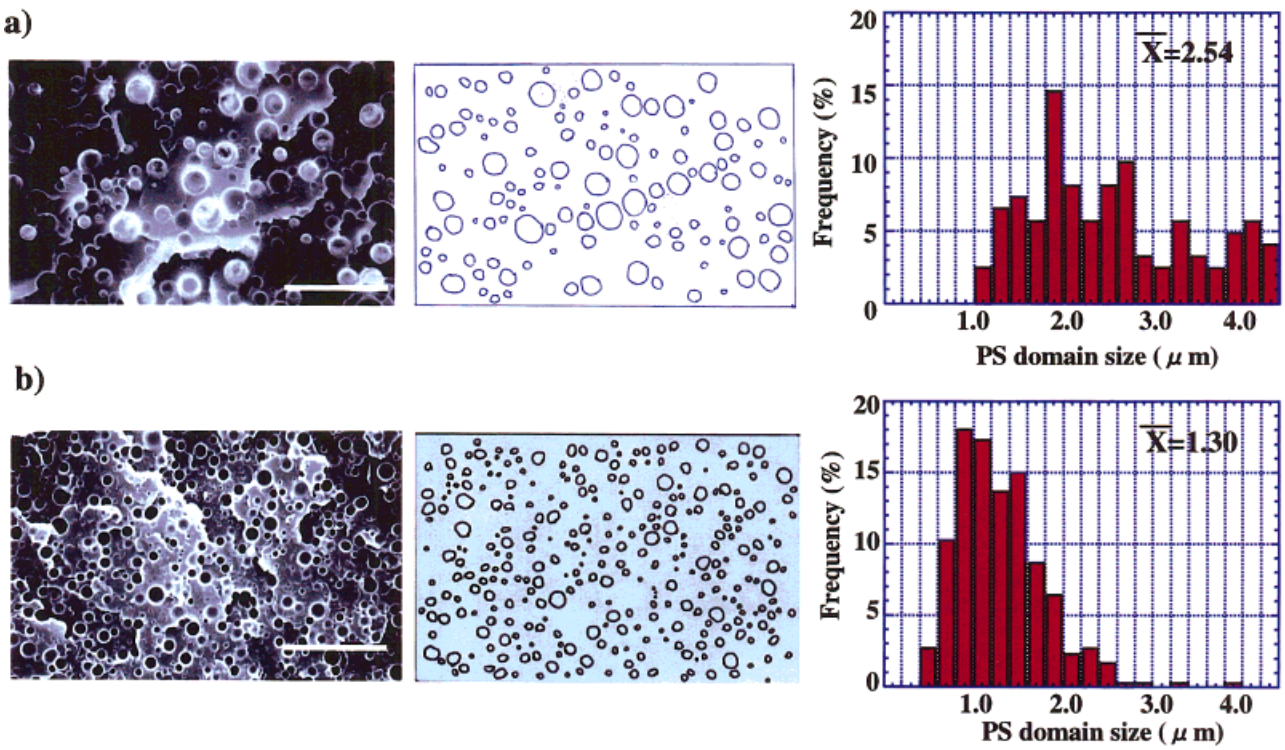


**Figure 6** SEM micrographs, binary images, and the PS domain size distributions of the HOOC–PS–COOH/PC blends: (a) HOOC–PS–COOH/PC (15/85); (b) HOOC–PS–COOH/PC/PS–PAr block copolymer (2185) (15/85/3 blends. The $M_n$ of the used HOOC–PS–COOH = 21,000. Bar in the SEM micrographs = 10 $\mu$m. [Color figure can be viewed in the online issue, which is available at www.interscience.wiley.com.]

The NMR spectra at 7.5–6.2 and 9.0–7.5 ppm in the HFIP solubles were assigned to the PS chains of reaction product 1 and the PAr component of product 1 or product 3, respectively. The increase of the NMR spectrum at 7.5–6.9 ppm in the HFIP insolubles was ascribed to the PAr/PC chains of product 2. In addition, the result of the mass balance showed the amount of the HFIP solubles increased after the melt mixing for run 2185/PC and 2170/PC blend. For the run 0870/PC blend the amount of HFIP insolubles increased. These results indicated that the generated amount of products 1 and 3 was greater than that of product 2 for the run 2185/PC and the 2170/PC blends. On the other hand, for the run 0870/PC blend the result was opposite. Because the generated PS–PAr/PC block copolymers were divided into both HFIP solubles and insolubles, depending on their PAr/PC composition, we could not estimate the degree of reactivity.

From these HFIP extraction results, PS–PAr block copolymers were demonstrated to react with PC under such a mild condition as melt mixing at 260°C without any catalyst. The degree of the reactivity of Figure 2 could not be estimated from these HFIP extractions, however.

### Phase Morphologies of HOOC–PS–COOH/PC and PS–PAr Block Copolymer/PC Blends

Figures 6 and 7 show phase morphologies, binary images, and the PS domain size distributions in the 15/85 blends of COOH–PS–COOH ($M_n$ = 21,000)/PC and PS–PAr block copolymer/PC, respectively. The morphologies of these blends seemed almost the same in their form and shape: the PS domains dispersed in the PC matrix and the shape of the PS domains seemed almost circular. There was a difference in the PS domain size and its distribution between them. In the HOOC–PS–COOH/PC blend, the PS domains were dispersed on the macroscale of 2.5 $\mu$m, on average [Fig. 6(a)]. When compatibilized with 3 wt % of the PS–PAr block copolymer (run 2185), the average size was reduced from 2.5 to 1.3 $\mu$m and its distribution also shifted to the smaller side [Fig. 6(b)]. These results indicated that the PS–PAr block copolymer could compatibilize the

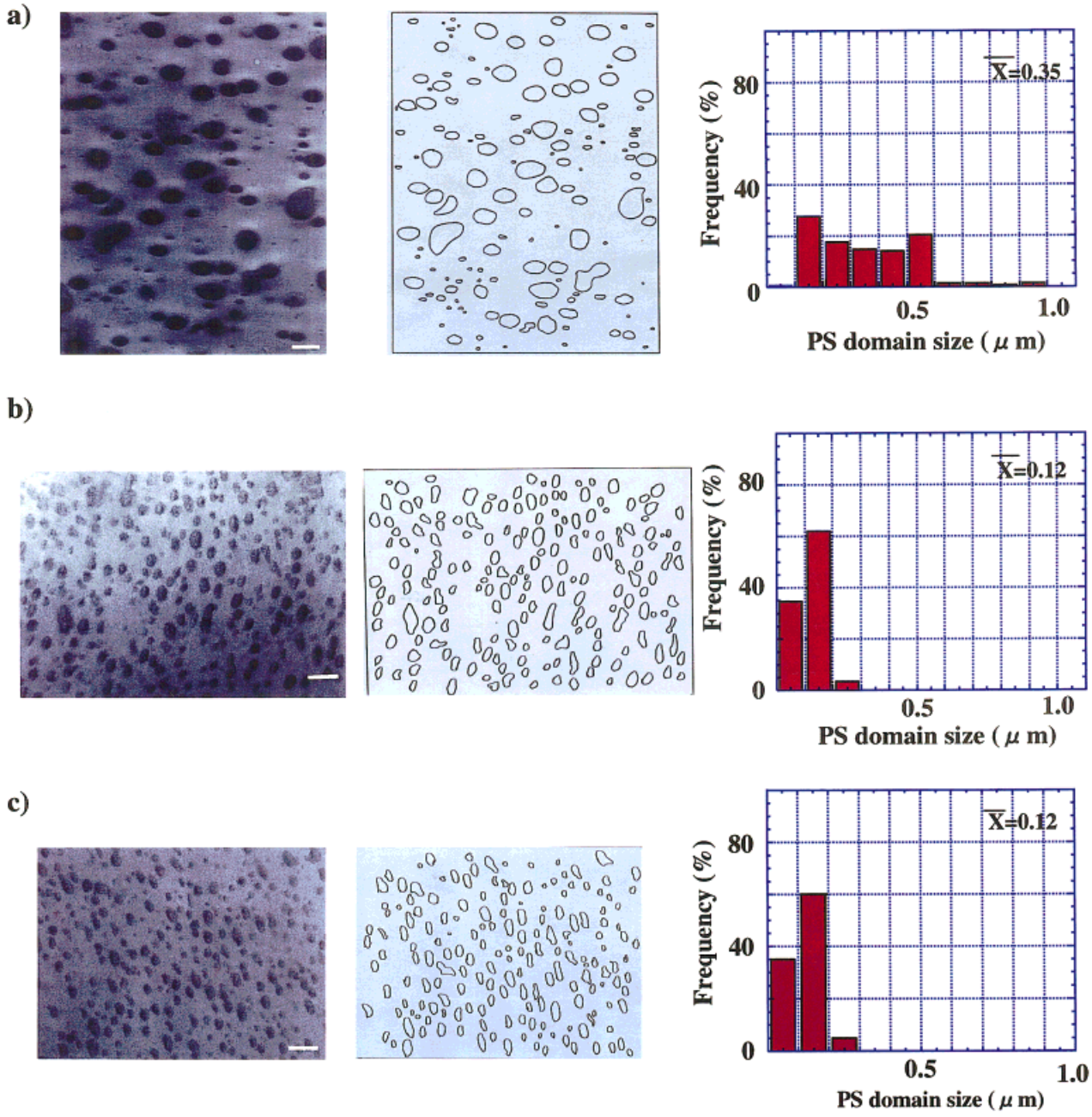


**Figure 7** TEM micrographs, binary images, and the PS domain size distributions of the PS–PAr block copolymer/PC blends. The 15/85 blends of (a) run 2185/PC, (b) run 2170/PC, and (c) run 0870/PC are shown. In TEM micrograph (a) bar = 500 nm; in TEM micrographs (b) and (c) bar = 100 nm. [Color figure can be viewed in the online issue, which is available at www.interscience.wiley.com.]

HOOC–PS–COOH/PC blend to some extent. However, even compatibilized with 3 wt % of the PS–PAr block copolymer, the PS domain size and its distribution in the COOH–PS–COOH/PC blend could not be reduced to smaller than the visible light wavelength (400–800 nm).

In the PS–PAr block copolymer/PC blends the PS domain size was reduced, on average, to be smaller than the visible light wavelength because of the chemical bonding between PS and PC chains. In particular, when PC was blended with either run 0870 or run 2170, the distribution of

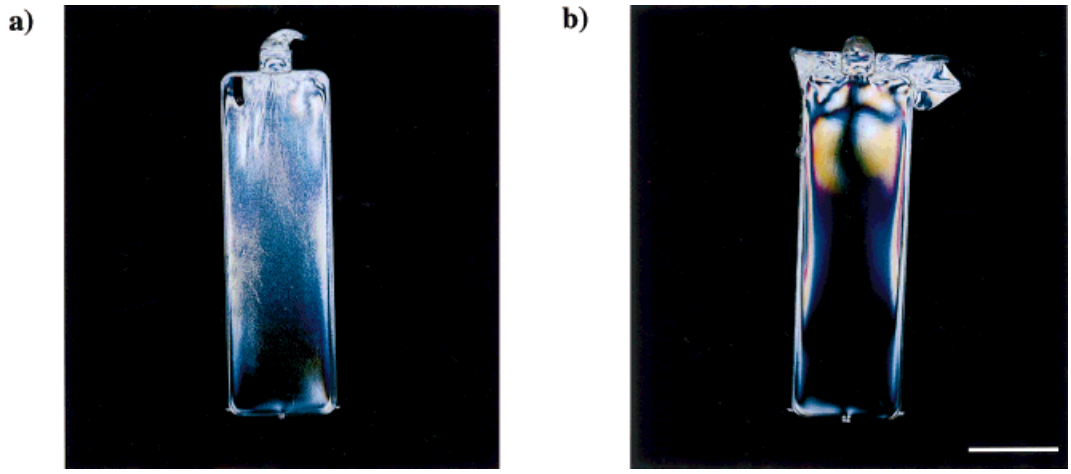


**Figure 8** Fluctuation of birefringence. The 15/85 blends of (a) HOOC–PS–COOH ($M_n$ = 21,000)/PC and (b) run 2185/PC are shown. (The specimens were inserted between the crossed nicols polarizing plates.) Bar = 10 mm.

PS domain size sifted smaller than that of the run 2185/PC blend. In these blends the PS domains were completely reduced to a smaller size than the visible light wavelength [Fig. 7(b), (c)]. These differences in the PS domain size and its distribution were supposedly attributed to the differ-

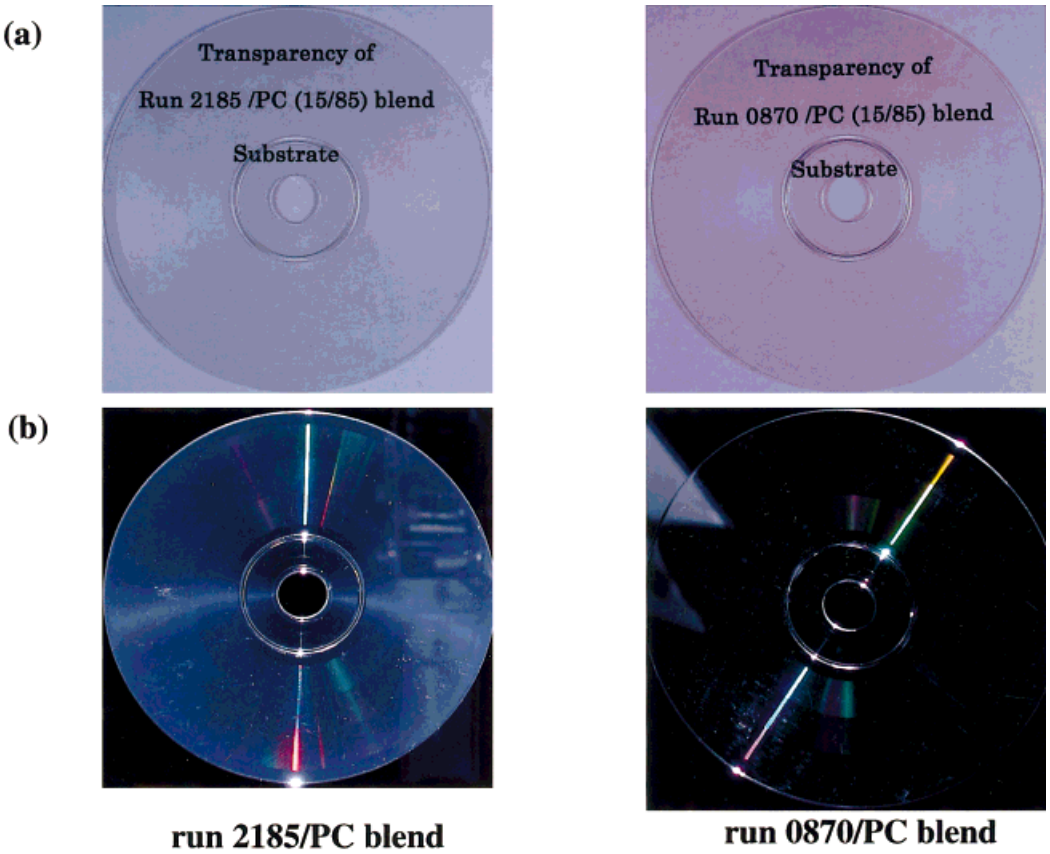


**Figure 9** Transparency of the PS–PAr block copolymer/PC blend substrates. Substrates were placed on white plates (a) and on reflective plates (b).

**Table IV Transmissivity of PC, HOOC–PS–COOH/PC, and PS–PAr Block Copolymer/PC Blends**

| | PC | HOOC–PS–COOH/PC | Run 2185/PC | Run 0870/PC | Run 2170/PC |
|---|---|---|---|---|---|
| 400 nm | 86 | 56 | 70 | 85 | 85 |
| 800 nm | 88 | 70 | 80 | 89 | 87 |

[a] Values are expressed as percentages.

ence in the PAr composition in pure PS–PAr block copolymers. As shown in the Table I, the PAr composition in pure PS–PAr block copolymer of either run 0870 or run 2170 was almost twice that of run 2185. As a result, the degree of reactivity between pure PS–PAr block copolymer and PC should be higher for either the run 0870 or the run 2170/PC blends than that for the run 2185/PC blend.

## Birefringence Fluctuation and Transparency of HOOC–PS–COOH/PC and PS–PAr Block Copolymer/PC Blends

### *Birefringence Fluctuation*

Figure 8 compares optical homogeneity between the HOOC–PS–COOH/PC and the run 2185/PC blends observed under polarizing light. The HOOC–PS–COOH/PC blend seemed heterogeneous on the real scale, whereas the run 2185/PC blend seemed homogeneous. These differences were supposedly the result of the difference in the dispersed domain size. As described previously,[9] in the immiscible polymer blend system, the retardation should be different between the matrix and the inside of the dispersed domains because of the difference in the intrinsic birefringence or the stress and the relaxation history of the constituent polymers during the injection-molding process. Given that in the HOOC–PS–COOH/PC blend the dispersed PS domains were all larger than the visible light wavelength, these difference could be observed as a birefringence fluctuation[49] on the real scale. On the other hand, in the run 2185/PC blend this birefringence fluctuation could be hardly observed because the size of the dispersed PS domains was smaller, on average, than the visible light wavelength.

### *Transmissivity*

Table IV shows the transparency of the PC, the HOOC–PS–COOH/PC, and the PS–PAr block copolymer/PC blends substrates. Each sample showed a little higher transmissivity at the wavelength of 800 than that at 400 nm. The transmissivity of these blends increased as the PS domain size and its distribution decreased: the transmissivity increased in the order of the run 0870/PC, the run 2185/PC, and the HOOC–PS–COOH/PC blend. For the run 0870/PC blend the transmissivity reached a value almost equal to that of the PC at both wavelengths. However, dependence of the transmissivity on the dispersed domain size was not as strong as the case for the PS–PAr blend system.[9] The HOOC–PS–COOH/PC blend showed a transmissivity of 70% at 800 nm, in spite of the large average size of the PS domain (2.5 $\mu$m), although the PS–PAr blend was no longer transparent when the average size of the dispersed domain surpassed 1.0 $\mu$m.[9]

Figure 9 compares the transparency of the run 2170/PC and the run 0870/PC blend substrate on both white and reflective plates. Although the run 2185/PC blend was fully transparent on the white plate, it seemed cloudy on the reflective plate. On the other hand, the run 0870/PC blend maintained optical clarity not only on the white but also on the reflective plate.

The transparency of these blends can be explained by eqs. (2)[50] and (3):

$$\alpha = 2\pi^3(\Delta n_{m/s}/n_m)^2 V_s \phi_s/\lambda^4 \quad (2)$$

$$T\% = k\ \exp(-\alpha d) \quad (3)$$

where $\alpha$ is the absorbance coefficient; $n_m$ is the refractive index of the matrix; $\Delta n_{m/s}$ is the difference in the refractive indices between matrix and the scattering objects; $V_s$ and $\phi_s$ are the volume and volume fraction of the scattering objects, respectively; $\lambda$ is the wavelength of the incident beam; and $d$ is the specimen thickness. From eq. (2), as $\lambda$ becomes smaller, $\alpha$ increases. Correspondingly, the transmissivity became smaller at $\lambda$ = 400 nm than at 800 nm for each sample. In addition, as the size and the distribution of the dispersed PS domains became larger, $V_s$ and $\phi_s$ in eq. (2) increased, resulting in lower transmissiv-

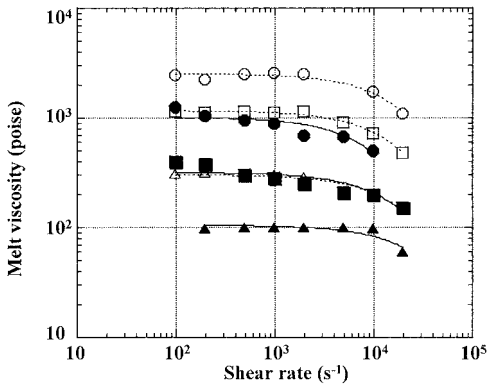


**Figure 10** Melt viscosity versus shear rate. ○, □, and △ represent PC at 270, 300, and 330°C, respectively; ●, ■, and ▲ represent run 0870/PC blend at 270, 300, and 330°C, respectively.

ity. Because $\Delta n_{m/s}$ of these blends was much smaller than that of PS and PAr blend system ($\Delta n_{PS/PC} = 0.006$[50]), $\Delta n_{PAr/PS} = 0.02$[8]), dependence of the transmissivity on the average size of the dispersed domain was extremely smaller for the blend system of the PS/PC than that for the PS/PAr.[8] Furthermore, when the substrate was put on the reflective plate, the light passing through the substrates was doubled. From eq. (3), this affected the transmissivity in the same way in which $\alpha$ was doubled. In the run 2185/PC blend, the PS domain size was smaller, on average, than the visible light wavelength, although its distribution was not reduced to this level. As a result, although $\alpha$ by itself was small, the doubled value of $\alpha$ was not small enough to maintain optical clarity, whereas in the run 0870/PC blend, whose PS domains were completely controlled to be smaller than the visible light wavelength, $\alpha$ should be small enough even if it were doubled.

In the higher-density optical storage system, the polarized laser beam with $\lambda = 400$ nm, which passes through the substrate and is reflected on the substrate surface, deflects the optical signal. Thus, the homogeneity under the polarizing light, the clarity on the reflective plate, and the transparency at 400 nm are required. Considering these experimental results combined with the results of the morphology analysis, we could conclude as follows. The PS domain should be controlled to be completely smaller than the visible light wavelength to attain the practical transparency for optical disk application by blending PS and PC. In our experimental system, for this purpose, PS should be copolymerized with PC through the reaction of Figure 2 by adjusting PAr wt % in the fed PS–PAr block copolymer to around 30 wt %.

## Melt Viscosity and Retardation of PS–PAr Block Copolymer/PC Blend and PC Substrates

Figure 10 gives the melt viscosity data of the run 0870/PC blend as a function of shear rate. By blending PC with 15 wt % of the PS–PAr block copolymer, the melt viscosity was lowered to a value almost equal to that of PC at about 30°C higher temperature.

Figures 11 and 12 show how the normal retardation in the substrates of the run 0870/PC blend and the PC depended on the melt temperature and the mold temperature, respectively. The retardation dependence on these factors was very similar between the PC and the run 0870/PC blend. At lower melt temperature, the retardation was a decreasing function of the melt temperature and the radial position. They showed relatively large positive values induced by the retained orientation of the PC molecules. At higher

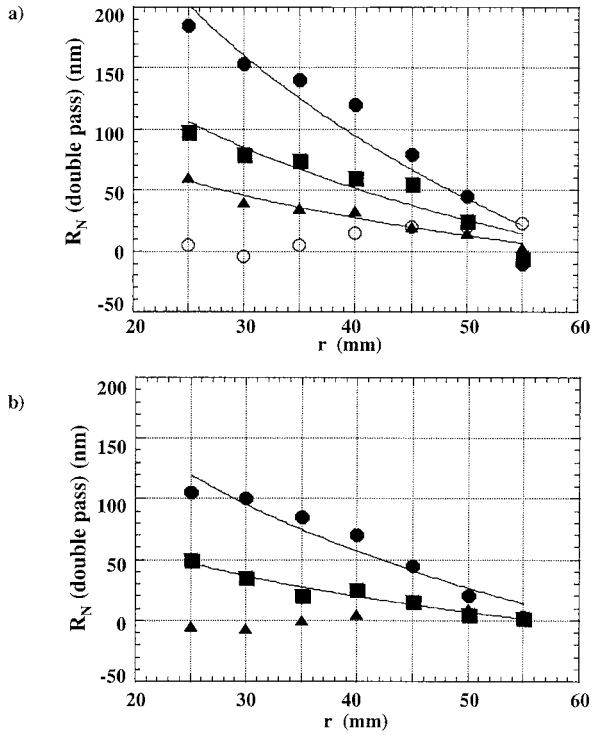


**Figure 11** Radial profile of the normal retardation in the disk substrate as a function of the melt temperature when the mold temperature was 100°C: (a) PC and (b) run 0870/PC blend substrate. Melt temperatures were 300, 320, 340, and 370°C, represented by ●, ■, ▲, and ○, respectively.

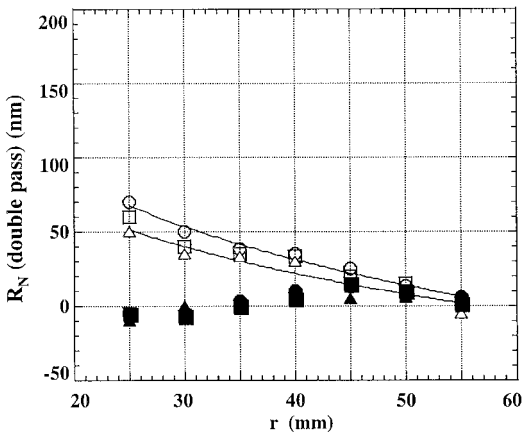


**Figure 12** Radial profiles of the normal retardation in the disk substrates as a function of the mold temperature when the melt temperature was 340°C. ○, □, and △ represent $R_N$ of PC at the mold temperature of 80, 100, and 120°C, respectively; ●, ■, and ▲ represent $R_N$ of the run 0870/PC blend at the mold temperature of 80, 100, and 120°C, respectively.

melt temperature the retardation was reduced to almost 0, although several reversals in the sign of the retardation were observed by the packing effect.[51] Dependence of the retardation on the mold temperature was less pronounced for both run 0870/PC blend and PC.[19–21]

Because the PS composition (10.5 wt %) in the run 0870/PC blend was much smaller than the reported birefringence free point (40 wt %)[50,51] of PS/PC blend, positive and negative birefringence of PC and PS should not be fully compensated. However, because of the lowered melt viscosity in Figure 11 the degree of molecular orientation should be reduced during the substrate molding. As shown in Figure 12, the retardation of the run 0870/PC blend was almost equal to that of PC at 30–40°C higher melt temperature. The run 0870/PC blend could reduce the retardation profile within ±20 nm at the melt temperature of 330°C, whereas for PC a melt temperature higher than 370°C was necessary to attain such a small retardation profile. These results represented a potential that the process window for the substrate molding could expand to 30–40°C lower melt temperature by blending PC with 15 wt % of the PS–PAr block copolymer.

## Groove Transcription of PC and PS–PAr Block Copolymer/PC Blend Substrates

Figure 13 shows the degree of the groove transcription as a function of the melt temperature and the mold temperature. Figure 14 gives a typical AFM picture of the replicated grooves at the melt temperature and the mold temperature of 340 and 100°C, respectively. For the run 0870/PC blend as well as PC substrates, the degree of the groove transcription was an increasing function of both melt and mold temperatures. The effect of the mold temperature was much more pronounced than that of the melt temperature. When compared at the same melt temperature or mold temperature, the degree of the transcription was much larger for the run 0870/PC blend than that for PC. In particular, at the mold temperature of 100°C and above, the transcription of the run 0870/PC blend was improved rapidly. At such mold temperatures, the degree of transcription reached more than 85%. On the other hand, the degree of transcription of PC reached 85% when the mold temperature surpassed 120°C. These results represented a potential that the PS–PAr block copolymer/PC blend could expand the process window for the substrate molding to 20°C lower temperature than that for PC.

The transcription behavior of the run 0870/PC blend and PC could be explained qualitatively by

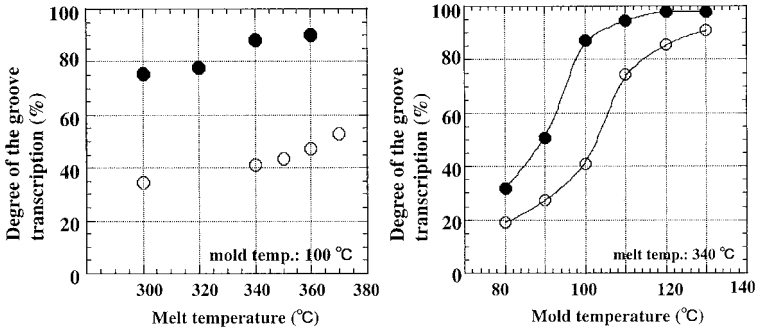


**Figure 13** Degree of groove transcription as a function of (a) melt temperature and (b) mold temperature: ○, PC; ●, run 0870/PC blend.

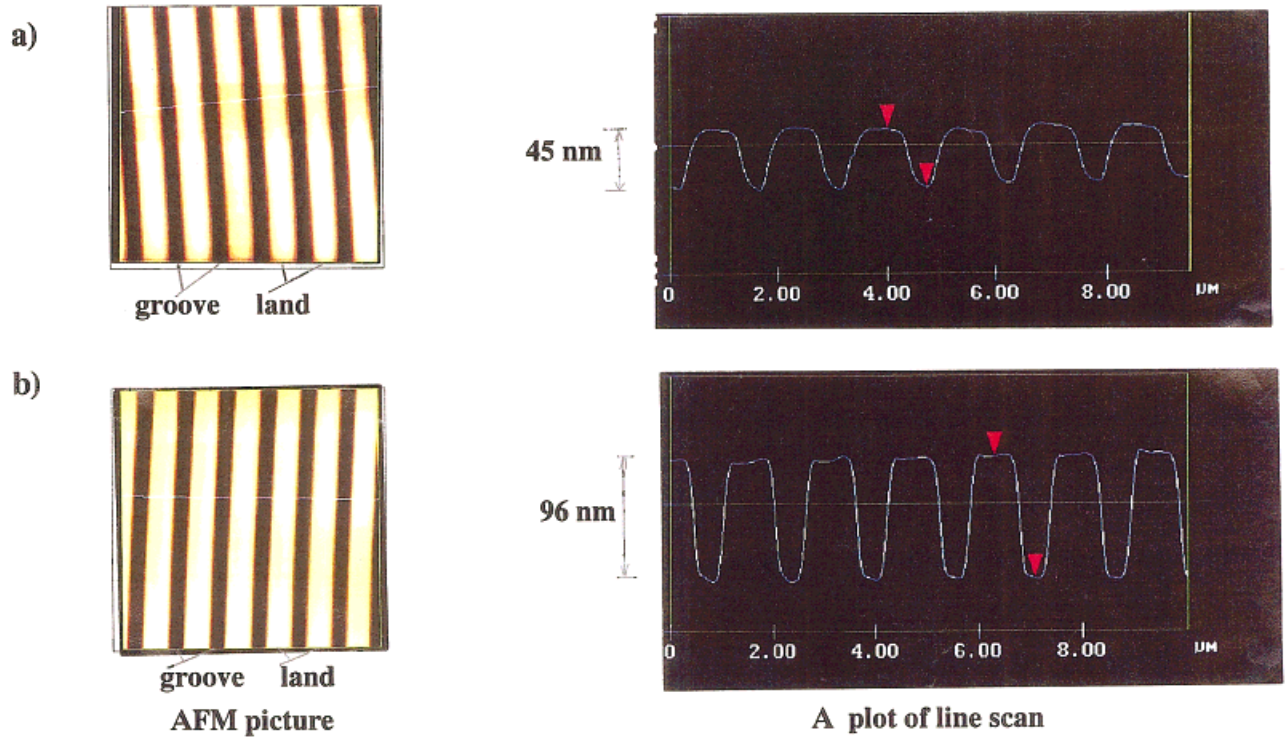


**Figure 14** AFM picture of the grooves replicated on the substrate surface. The substrates were injection molded at the mold temperature of 100°C: (a) PC and (b) run 0870/PC substrates. [Color figure can be viewed in the online issue, which is available at www.interscience.wiley.com.]

the creep deformation model proposed by Yoshii et al.[15–17] According to this model, the development of the groove transcription was caused by the creep deformation of the vitrified layer, and the degree of the transcription was subject to both heat transformation in the mold and deformation behavior of the vitrified layer. As the mold temperature or the melt temperature increased, the cooling rate and the resistance to the deformation was lowered. Consequently, the degree of the transcription increased with them for both the run 0870/PC blend and PC. In particular, as shown in Figure 15, the run 0870/PC blend showed two $T_g$'s: 116 and 156°C, corresponding to the PS- and the PC-rich phase, respectively. Because of the PS-rich phase, the elastic modulus of the blend was lowered around 100°C. As reported in Yoshii et al.,[17] the modulus of elasticity was one of the most dominant properties that determined the transcription development. Thus, because of the PS-rich phase, the vitrified layer in the run 0870/PC blend should be softened around 100°C and above. These features should lead to a rapid improvement of the transcription at these temperatures.

## CONCLUSIONS

1. The reactivity of the reaction scheme of Figure 2 was confirmed by comparing the chemical composition and the mass bal-

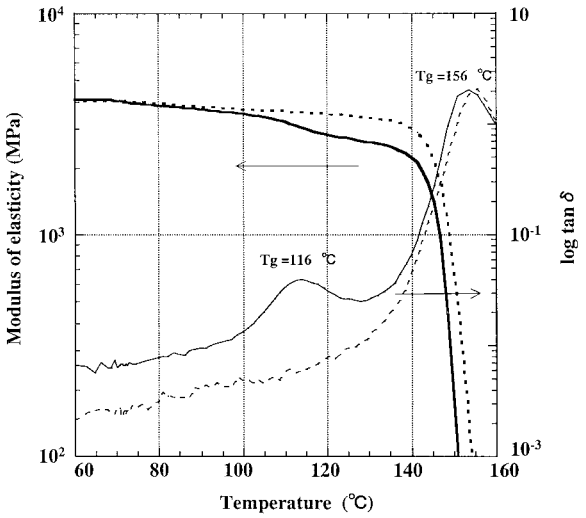


**Figure 15** Viscoelastic properties of the run 0870/PC blend (solid) and PC (dashed).

ance of the HFIP solubles and insolubles both before and after the reaction. The results of the HFIP extraction indicated that PS–PAr block copolymer could copolymerize with PC under such a mild condition as just melt mixing at 240°C without any catalyst.

2. Because of the chemical bonding between the PS and the PC chains, the PS domains in the PS–PAr block copolymer/PC blend could be reduced, on average, to a size smaller than the visible light wavelength. In particular, by adjusting PAr wt % in the fed PS–PAr block copolymer to 30 wt % in the reaction of Figure 2, the PS domain size could be completely reduced to be smaller than the visible light wavelength.
3. By controlling the PS domain size to be smaller, on average, than the visible light wavelength, the birefringence fluctuation could be reduced small enough to maintain the optical homogeneity under polarizing light. In addition, by controlling the PS domain size to be completely smaller than the visible light wavelength, the internal scattering in the blend substrate was reduced small enough to maintain transparency, even at 400 nm and on the reflective plate.
4. By blending PC with 15 wt % of the PS–PAr block copolymer, the melt viscosity could be lowered to the level of PC at about 30°C higher temperature. The lowered melt viscosity could reduce the retardation in the disk substrate by the degree corresponding to the disk made at 30°C lower melt temperature of PC. This result indicated a potential that the process window for the molding of PC substrate could be expanded to 30°C lower temperature.
5. The PS–PAr block copolymer/PC blend substrate could attain 85% of the groove transcription at about 20°C lower mold temperature than that of PC. This was supposedly attributed to the lowered elastic modulus caused by the PS-rich phase in the blend.
6. Because of its excellent transparency and a potential for process flexibility, the PS–PAr block copolymer/PC blend would be a promising material for higher-density disk substrates.

The authors thank K. Shimojo of Nippon Steel Co. for helping in the operation of disk substrate molding and the discussion of data.

## REFERENCES

1. Ceresa, R .J. Block and Graft Copolymers; Butterworth: London, 1962.
2. Aggarwal, S. L. Block Copolymers; Plenum: New York, 1970.
3. Paul, D. R. Polymer Blends, Vol. 2; Academic Press: New York, 1978; Chapter 12.
4. Yamatita, Y. Chemistry and Industry of Macromonomers; Tokyo IPC: Japan, 1984.
5. Akiyama, S.; Nishi, T.; Inoue, T. Polymer Blends; CRC Press: Boca Raton, FL, 1981; p. 169.
6. Ohishi, H.; Kimura, M. Nippon Steel Technical Rep 1993, 53, 39.
7. Ohishi, H.; Ohwaki, T.; Nishi, T. J Polym Sci Polym Chem Ed 1998, 36, 2839.
8. Ohishi, H.; Nishi, T. J Polym Sci Polym Chem Ed 2000, 38, 299.
9. Ohishi, H.; Kishimoto, S.; Nishi, T. J Appl Polym Sci to appear.
10. Ohishi, H.; Kishimoto, S.; Ikehara, T.; Nishi, T. J Polym Sci Polym Phys Ed 2000, 38, 127.
11. Ohishi, H.; Shimojoh, K.; Wada, K. 6th SPSJ IPC preprint 181, 1997.
12. Ohishi, H.; Ikehara, T.; Nishi, T. J Appl Polym Sci to appear.
13. Pisipati, R. M.; Newcome, J. M.; Lower, H. M. Plast Eng 1995, 4, 33.
14. Sato, I. Plast Age 1999, 45, 84.
15. Yoshii, M.; Kuramoto, H.; Kato, K. Kobunshi Ronbunshu 1992, 49, 703.
16. Yoshii, M.; Kuramoto, H.; Kato, K. Polym Eng Sci 1994, 34, 1211.
17. Yoshii, M.; Kuramoto, H.; Kato, K. Polym Eng Sci 1998, 38, 1587.
18. Greener, J.; Kesel, R.; Contesable, B. A. AIChE J 1989, 35, 449.
19. Siebourg, W.; Schmid, H.; Rateike, F. M.; Anders, S.; Lower, H. Polym Eng Sci 1990, 30, 1133.
20. Kanai, T.; Shibata, Y. Seikei Kakou 1990, 2, 2.
21. Yoshii, M.; Kuramoto, H.; Kaneda, A. Kobunshi Ronbunshu 1991, 48, 129.
22. Kunori, T.; Geil, P. H. J Macromol Sci Phys 1980, B18, 93.
23. Eastmond, G. C.; Haraguchi, K. Polymer 1983, 24, 1171.
24. Rundin, A.; Brathwaite, N. E. Polym Eng Sci 1984, 24, 1312.
25. Kim, W. N.; Burns, C. M. J Appl Polym Sci 1987, 34, 945.
26. Kim, W. N.; Burns, C. M. J Appl Polym Sci 1990, 41, 1575.

27. Mckay, I. D. J Appl Polym Sci 191, 42, 281.
28. Kim, C. K.; Paul, D. R. Macromolecules 1992, 25, 3097.
29. Kim, C. K.; Paul, D. R. Polymer 1992, 33, 4941.
30. Nishi, T.; Suzuki, T.; Tanaka, H.; Hayashi, T. Makromol Chem Macromol Symp 1991, 51, 29.
31. Majumdar, B.; Keskkula, H.; Paul, D. R. Polymer 1994, 35, 3165.
32. Majumdar, B.; Keskkula, H.; Paul, D. R. Polymer 1994, 35, 4263.
33. Majumdar, B.; Keskkula, H.; Paul, D. R. Polymer 1994, 35, 5468.
34. Maa, C. T.; Chang, F. C. J Appl Polym Sci 1993, 49, 913.
35. Lee, P. C.; Kuo, W. F.; Chan, F. C. Polymer 1994, 35, 5641.
36. Ritta, M.; Holsti–Meittinen, R. M.; Heino, M. T.; Seppala, J. V. J Appl Polym Sci 1995, 57, 573.
37. Kaifoglou, N. K.; Skafidas, D. S.; Kallitsis, J. K.; Lambert, J.-C.; Van der Stappen, L. Polymer 1995, 36, 4453.
38. Ito, Y.; Ogawa, H.; Ishida, Y.; Ohtani, H.; Tsuge, S. Polym J 1996, 28, 1090.
39. Wildes, G.; Harada, S.; Keskkula, H.; Janarthanan, V.; Paul, D. R. Polymer 1999, 40, 3069.
40. Wildes, G.; Keskkula, H.; Paul, D. R. Polymer 1999, 40, 5609.
41. Wildes, G.; Keskkula, H.; Paul, D. R. J Polym Sci Part B Polym Phys 1999, 37, 71.
42. Godard, P.; Dekonink, J. M.; Devlesaver, V.; Devaux, J. J Polym Sci Polym Chem Ed 1986, 24, 3301.
43. Suzuki, T.; Tanaka, H.; Nishi, T. Polymer 1989, 30, 1287.
44. Devaux, J.; Godard, P.; Mercier, J. P. J Polym Sci Polym Phys Ed 1982, 20, 1881.
45. Devaux, J.; Godard, P.; Mercier, J. P. J Polym Sci Polym Phys Ed 1982, 20, 1895.
46. Devaux, J.; Godard, P.; Mercier, J. P. J Polym Sci Polym Phys Ed 1982, 20, 1901.
47. Baro, A. M.; Vazquez, L.; Bartolame, A.; Gomez, J.; Garcia, N.; Goldberg, H. A.; Sawyer, L. C.; Chen, R. T.; Kohn, R. S.; Reifenberger, R. J Mater Sci 1988, 24, 1739.
48. Espinosa, E.; Fremdaz–Berridi, M. J.; Maiza, I.; Valeno, M. Polymer 1993, 34, 382.
49. Manabe, K.; Niwano, M. Kobunshi Ronbunshu 1991, 40, 679.
50. Hayakawa, S. Rikougaku-kisokouza; Asakura IPC: Japan, 1976; p. 24.
51. Greener, J. Polym Eng Sci 1986, 26, 886.